Initial stages of pollutants dispersion around municipal waste disposal facilities: a case study in Northern Portugal

J. Figueiras*, M.A. Gonçalves and A. Mateus

Faculdade de Ciências,
Department of Geology and CREMINER,
Universidade de Lisboa,
Ed. C6, Piso 4, Campo Grande,
1749-016 Lisboa, Portugal
Fax: +351-217500064
E-mail: jmvf@fc.ul.pt
E-mail: mario.goncalves@fc.ul.pt
E-mail: amateus@fc.ul.pt
*Corresponding author

F.O. Marques

Faculdade de Ciências,
Department of Geology and LATTEX (presently CGUL),
Universidade de Lisboa,
Ed. C6, Piso 4, Campo Grande,
1749-016 Lisboa, Portugal
Fax: +351-217500064
E-mail: fomarques@fc.ul.pt

F. Monteiro Santos

Faculdade de Ciências,
Department of Physics and CGUL,
Universidade de Lisboa,
Ed. C8, Piso 3, Campo Grande,
1749-016 Lisboa, Portugal
Fax: +351-217500064
E-mail: fasantos@fc.ul.pt

R. Mota

Department of Geotechnics,
Laboratório Nacional de Engenharia Civil,
Avenida do Brasil, 101,
1700-066 Lisboa, Portugal
Fax: +351-218443021
E-mail: rmota@lnec.pt

Abstract: The combined use of several geological, geochemical and geophysical observations during six years enabled the detection of a very faint halo of chemical contamination induced by the operation of a young waste disposal facility in Northern Portugal. The halo does not classify as pollution by any standards, but is observed to be intensifying and thus signals a potential hazardous situation in future years. The approach used shows that a comprehensive and diverse monitoring programme, although relatively inexpensive and easy to carry out, may detect concealed leaks long before any environmental concern is justified, and thus may help avert future complex remediation needs caused by the uncontrolled growth of undetected underground pollution plumes.

Biographical notes: Jorge Figueiras earned his PhD in 1997 from the University of Lisbon, where he is now an Assistant Professor. His research work centres on environmental geochemistry, and he has published several papers on metal dispersion around landfills. He also works on metal geochemistry dispersed around ancient mining centres.

Mário A. Gonçalves has graduated in Geology (1989) and received an MSc (1996), and a PhD (2004) in Geology from the University of Lisbon. His research interests are mainly in the field of environmental geochemistry and mineralogy, especially in the study of the adsorption mechanisms of metals on mineral surfaces. He also developed some studies on process modelling (geochemical, fractal and geostatistical). Currently, he is Assistant Professor at the Department of Geology in the Faculty of Sciences of the University of Lisbon.

António Mateus obtained his Geology and PhD (Geology – Metallogeny) in 1985 and 1995, respectively, from the University of Lisbon. Currently, he is a full time Professor of the Faculty of Sciences at the University of Lisbon. His research interests cover different topics, mostly in interface fields between mineralogy, geochemistry, ore-forming processes, rock deformation and fractals in geosciences. He is a member of SGA, MSA, SGP and APG.

Fernando Ornelas Marques received his BSc in Geology in 1986 and his PhD in Geodynamics in 1994 from the University of Lisbon. He is presently an Aggregate Professor in the Department of Geology, University of Lisbon, Portugal. His research interests are mainly related with structural geology, tectonophysics and geodynamics, but also include hazardous waste handling and disposal, and site monitoring. His research has been published in international journals. He is presently a member of the Editorial Board of *Tectonophysics*.

Fernando Monteiro Santos received his PhD in Physics (Geophysics) from the University of Lisbon in 1994. Since July 1994, he is an Assistant Professor at the Physics Department of the Lisbon University. His main interests are electromagnetic exploration methods, including applications in continental tectonics, mining and environmental studies. He is an associated editor of *Geophysical Prospecting* and is a member of AGU and SEG.

Rogério P.V. Mota received his Degree in Geophysics from the University of Lisbon in 1990, MSc in Geophysics from University of Lisbon in 1993, PhD in Geophysics at the University of Lisbon in 2007. Since February 1993, he is a research assistant at the Geotechnics Department of the National Laboratory of Civil Engineering (LNEC). His main interests are seismic and resistivity surveys applied to shallow investigation of environmental and geotechnics problems, cross-hole seismic testing for site characterisation and pile testing (sonic and cross-hole). Investigation Award "Augusto Vieira da Silva" from Lisbon Town Council for his MSc thesis. He is a member of SPG and EAGE.

1 Introduction

Modern municipal waste disposal facilities are engineered to minimise the emission of harmful chemicals to the surrounding environment (Stengele and Plötze, 2000). This is achieved by dumping the waste on a multi-layer impervious bottom liner and by covering the waste piles as soon as possible with a suitable composite layer that will isolate the disposed off waste from the environment. However, the isolation provided by both bottom and top liners is quite likely to be ineffective in the long run, which means that the dumped waste or its alteration products may end up in the surrounding environment. Excellent accounts on these issues can be found in Christensen et al. (2001) and Bjerg et al. (2003).

Since the beginning of the 1990s, Portugal has shifted from uncontrolled dumping of municipal waste on the natural ground to concentrated deposition in newly built facilities. There are several of these facilities in Portugal that have been operating for a few years, and each of them provides an excellent natural laboratory for the study of the early stages of chemical dispersion around waste disposal sites. In this work, we report such a study for a facility that has been operating for eight years now and is located in Northern Portugal on an almost unaltered but heavily fractured granite basement, in a rugged, rainy ($\approx$1700 mm y^{-1}) region. We carried out a multidisciplinary study, which included:

- integration of multi-scale structural mapping

- fine fracture characterisation

- geophysical surveys (Wenner resistivity array profiles, VLF-EM method)

- chemical and structural characterisation of supergene mineral assemblages (and its adsorbed layers) occurring in altered rocks, soils, sediments and fracture fillings

- geochemical surveys of soils, sediments and ground and surface waters occurring in the immediate vicinity of the facility.

The results obtained made it possible to draw a clear picture of the contaminated plume long before any pollution is readily recognisable or any regulatory limit is reached or even approached. This work shows that an array of comparatively low-cost monitoring techniques can give an accurate picture of the situation around very young landfills, even when the environmental conditions differ but very little from the regional background, and can be used to detect latent hazardous situations.

2   Geological setting

The studied facility collects about 100,000 tons·y^{-1} of municipal and low hazard industrial waste produced by a population estimated at 275,000 people. It is located in NW Portugal, almost on top of a granite ridge ($\approx$450 m above sea level), at a site with mild temperate oceanic climate and high rainfall distributed all-year round except in summer. Very poor soil development prevents the agricultural use of the ridge, which is covered with natural vegetation and eucalyptus plantations. The facility extends from the ridge top down its steep southern flank half-way to an important stream running in a deeply incised valley; a hollow excavated in the ridge flank by an ephemeral creek running in a geological fracture has been chosen as the most convenient topographic setting for dumping. Most of the dumping surface is, thus, quite steep and tends to collect in-falling water to its median line, instead of allowing diffuse run-off to its edges.

Local soils are thin and immature, with regolith at the surface or a few centimetres deep. The geological basement is rather homogeneous and consists of a two-mica (mainly biotitic) granite with alkali feldspar megacrysts. Apart from micas, accessory minerals include monazite, chlorite and clay minerals, mainly resulting from feldspar weathering. The abundance and the size of feldspar megacrysts is somewhat variable and seems to correlate negatively with the distance to some of the most important shear zones that cut the granite and show evidence of late reactivation.

Fracturing is intense and observable at all scales. At the regional scale (Figure 1(A)), the most prominent fracture system strikes ENE-WSW and is responsible for parallel very wide valleys drained by major rivers. At this scale, the ridges separating these main valleys have low fracture density, so, valley excavation may be due to differential erosion induced by weathering differences caused by different fracture densities. However, it has been demonstrated (Marques et al., 2001) that at least the main valley bordering the facility ridge to the north is a graben resulting from the alpine stress field. Besides this most important fault system, two other prominent fault systems striking approximately NNW-SSE and E–W are present and show up clearly in the morphology of the highlands to the east of the facility.

At the local scale, the structural framework of these rocks is still characterised by a dense network of fractures (Figure 1(B)). Similar fracture orientations can be found at this more detailed scale and it can be shown that most of the structural discontinuities are indeed faults and not mere joints. Parallel faults are unevenly spaced and many of the most important fault zones have multiple traces; both circumstances cause considerable spatial variation of fracture density. Fracture fillings are usually absent or poorly developed; when present, their mineral assemblages range from

- high-temperature, hydrothermal mineral assemblages (quartz, tourmaline, muscovite and chlorite, sometimes also pyrite), showing strong strike-slip deformation in semi-brittle to brittle regimes, to

- low temperature fault gauges consisting of powdered granite, powdered earlier high-temperature mineral assemblages and clay minerals (mainly kaolinite and illite), vertically striated.

Faulting was, thus, generated during the latest stages of granite emplacement and cooling and has been later reactivated by alpine stresses (Marques et al., 2002).

Figure 1 Map of the main fractures and faults originally at 1 : 25000 scale mapping (A), and map of fractures and faults in the vicinity of the landfill facility originally at 1 : 10000 scale mapping (B). The fractures in B correspond only to the ones observed at the outcrop level and representative at the scale considered. Location of resistivity surveys (C); the landfill perimeter is also marked (see online version for colours)
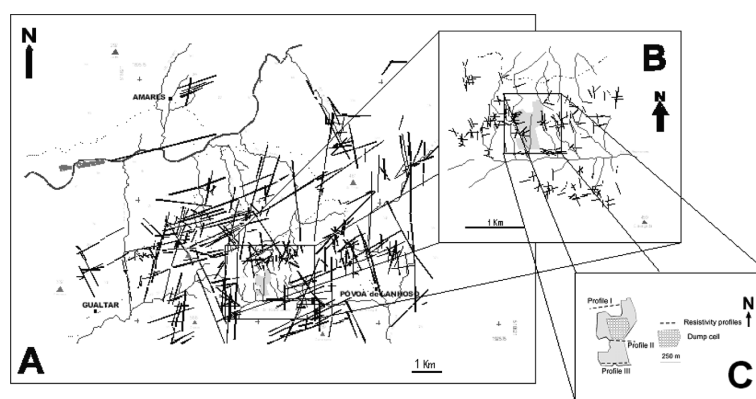
At the outcrop level, fracturing is again ubiquitous, fracture density being extremely variable from one location to another. In each outcrop, most (or all) of the regional structural strikes are present, crossing one another. At the hilltop outcrops, fracture density is generally low, with only a handful of fractures in several square metres of outcrop. Elsewhere, fracture density may be so high that non-fractured domains have linear dimensions not exceeding a few centimetres. Fracture density varies continuously between these two extreme cases. In general, outcrop fracture density is related to the local tectonic setting, the most densely fractured outcrops being located at points where two or more fault zones intersect; medium fracture density outcrops are usually located in the vicinity of mapped fault zones or inside multi-trace fault zones. Finally, it should be noted that many outcrops display conspicuous open fractures, some with textural evidence for early ductile to semi-ductile movement along their planes, sub-parallel to the present topographic surface. The tectonic significance of these structures is uncertain, but their relevance to shallow groundwater circulation cannot be overemphasised.

Overall, the fracture and fault pattern observed is self-similar (in a geometrical sense) at all scales (Mateus et al., 2003), which means that low-scale structural studies can be used to determine the local fracturing statistical parameters, even at sites where outcrop quality precludes a proper in situ characterisation.

The facility is located on a low fracture density domain, but fracturing is high in its immediate vicinities, especially downhill to the SE, where the presence of one of the

main ENE-WSW faults seems to have caused intense alteration of the granite and is responsible for the occurrence of several aligned intermittent springs. This positive correlation between fracture density and weathering intensity is expectable and indeed regionally observed. Since there is ample geomorphic evidence for the facility to have been built over a fracture zone, the granite basement under the dumping cells may be affected by a fairly high degree of alteration and its total permeability may be high, because of the general lack of fracture fillings regionally observed. During alteration, feldspars are partially or totally hydrolysed and converted to sheet silicates, but the alteration styles normally lead to a sandy texture, the cases of impervious strongly kaolinitised granites being quite rare. Also, at the facility location, soil does not behave as a natural impervious barrier, not only because of its natural thinness and sandy character but also because it was stripped, together with the most altered granite domains, before construction of the bottom liners.

3   Geochemistry

In a young facility such as the one under study, environmental variables around the facility are almost identical to the natural background. Therefore, the detection of any induced environmental chemical modification must rely on the detailed examination of a very diverse set of samples and on careful comparison of equivalent samples collected at places affected and unaffected by the facility operation (Figure 2).

Figure 2   (A) Sampling map of the surface and ground waters and (B) sampling map of the soils, sediments, and granite rocks
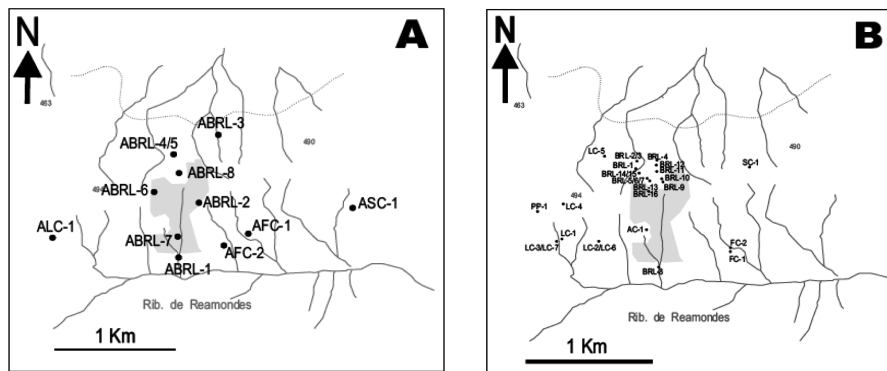
3.1   Sampling methods

Soils and thick sediments were collected by coring with aluminium tubes until the granite bedrock or the total work length of the tube was reached. Soil cores were extracted from the tubes and their 0.5 cm outer circular corona was discarded to avoid aluminium contamination. For soils thicker than 15 cm, the organic rich upper soil, grossly corresponding to the B horizon, was separated from the lower C horizon for chemical analysis. The creek sediments were collected dry by picking the few top cm layer. Soils were dried in the laboratory when necessary, and sieved to retain only the size fraction below 2 mm (Ure, 1995). Sediments were sieved to separate into two size

fractions corresponding to the range 90–63 µm (FS references), and <63 µm (FA references). The coarser sediments (T samples), generally corresponding to about 10 cm thick accumulations, were sieved to obtain a size fraction below 2 mm. All the remaining material was discarded. Altered and non-altered granite was crushed and ground to powder with an agate mortar. The same procedure was used for the soils and sediments with size particles up to 2 mm.

Water samples were collected using high-density polyethylene flasks. Samples of 2 L of water collected for analysis of major cations and anions were stored at most one day in the laboratory. Samples of about 100 mL of these same waters were collected for analysis of trace elements, 0.5 mL of reagent grade HNO_3 being added for solution stabilisation prior to analysis. Although care was taken to collect samples both at winter and summer times, most of our work coincided with intense drought conditions, which blurred the distinction between winter and summer samples. In fact, most of the samples collected in campaigns 4–6 already reflect abnormal hydrological conditions, shown by a general decrease in springwater flow leading to complete drying of many springs before the last sampling campaign.

3.2   Analytical methods

The analysis of major anions and cations of the water samples was performed in the laboratories of Instituto Superior Técnico (analytical techniques as in Table 1). Trace elements were analysed in Activation Laboratories (Canada), by ICP-MS. The main physical–chemical parameters were measured in the field. Electrical conductivity and temperature measurements were performed with a WTW LF91 conductivity meter using a WTW KLE 1/T cell coupled with a calibrated temperature probe. Both pH and Eh were measured with a WTW pH323 pH meter using a WTW SenTix 50 Ag/AgCl electrode (pH), and an E56 with a Pt and a reference Ag/AgCl electrode (Eh). The measured Eh values were then corrected for the standard H potential.

Chemical analyses of rock, soil and sediment samples were carried out in Activation Laboratories (Canada). Soil and sediments were analysed by Instrumental Neutron Activation Analysis (INAA) and Inductively Coupled Plasma (ICP-MS) using a four acid (HF, $HClO_4$, HNO_3 and HCl) digestion technique. Granite samples were fused with a lithium metaborate/tetraborate flux and analysed by ICP-MS.

A number of selected soil samples were also analysed for their moisture content, pH, conductivity, and organic carbon content, following standard determinative methods (e.g., Sheppard et al., 2000).

X-ray powder diffraction (Philips PW1710 diffractometer, PW1820 Bragg-Brentano goniometer, graphite crystal monochromator and Cu-K$_\alpha$ radiation) was used to characterise the mineralogy of the fine fraction of soils, sediments, and fracture fillings. Distribution and speciation of selected metals in sediments was assessed by sequential extraction techniques (Tessier et al., 1979; Hirner, 1992, 1996), and an extensive experimental study including electron microscopy and µ-PIXE (Gonçalves et al., 2002).

Table 1   Chemical composition of waters and leachate for selected major and minor elements

Ref.	Method	T	pH	Cl⁻	SO₄²⁻	HCO₃⁻	NO₃⁻	Na⁺	K⁺	Ca²⁺	Mg²⁺	SiO₂	Al	Mn	Fe	Cu	Zn	As	Br	I	Pb
		°C		IC	IC	POT	IC	FP	FP	FAA	FAA	MAS	ICP	ICP	ICP	ICP	ICP	ICP	ICP	ICP	ICP
				mg/L	mg/L	mg/L	mg/L	mg/L	mg/L	mg/L	mg/L	mg/L	µg/L	µg/L	µg/L	µg/L	µg/L	µg/L	µg/L	µg/L	µg/L
ABRL-1-1	s	17.8	6.07	8.3	0.8	21.4	5.5	7.7	1	3.96	1.54	8.9	94	360	2,390	<0.2	4.9	10.5	528	433	<0.1
ABRL-2-1	g	14.1	4.56	4.9	0.7	14.2	1.5	7.6	0.5	1.43	0.74	21.4	1,430	23.7	2,280	50.1	191	4.88	14	64	41.9
ABRL-3-1	s	14.3	5.64	5.7	0.8	6.6	2	4.4	<0.2	3.95	0.386	8.5	100	2.6	71	<0.2	5.7	0.14	9	15	0.5
ABRL-4-1	s	17.5	6.59	15.7	4.7	67.4	<0.3	10.7	7.7	19.9	1.31	-	354	77.4	839	11.4	39.1	1.97	41	12	3.4
ABRL-6-1	g	14.0	4.20	6.9	2	18.4	2.2	6.4	0.4	4.85	1.05	13.6	1,840	292	1,130	9.5	21.4	2.47	49	39	3.4
ABRL-7-1	l	N.A.	7.00	3000	253	14,500	<8	2400	1900	660	293		2,160	21,700	17,600	43	2,260	92	6,390	1,720	15
ABRL-8-1	g	15.5	5.30	4.9	4.1	30.3	1.4	8.4	0.6	5.7	1.79	18.5	72	23.6	751	3.5	9.9	18.7	45	10	1.7
AFC-1-1	g	13.8	4.43	4.9	0.9	4	2.2	4	0.3	0.66	0.381	8.5	195	6.1	<5	0.3	6.3	0.09	11	<1	0.2
AFC-2-1	g	13.3	4.50	5	0.4	6.4	2.5	5.2	0.5	0.78	0.429	10.1	332	16.9	45	<0.2	3.2	0.60	18	<1	0.3
ASC-1-1	g	17.3	4.37	5	0.9	4.1	2.5	4.4	0.3	0.68	0.396	8.8	148	5.7	<5	<0.2	<0.5	0.08	14	<1	<0.1
ALC-1-1	s	12.7	5.20	4.6	1	5.9	0.3	4	<0.2	0.48	0.34	9.5	94	1.6	23	<0.2	<0.5	0.07	11	<1	<0.1
ABRL-1-2	s	11.8	6.20	8.6	2.1	26.9	5.1	8.1	1.4	3.09	1.27	6.2	177	782	1,160	1.2	5.3	3.12	317	99	0.8
ABRL-2-2	g	13.8	4.00	4.2	1.4	3.2	1.6	3.2	<0.2	0.85	0.344	6.8	3,950	77.8	2,520	10.0	46.6	1.68	33	13	11.6
ABRL-3-2	s	11.8	5.40	3.9	0.9	3.3	0.9	2.8	<0.2	2.78	0.303	5.9	138	3.7	85	0.8	1.1	0.14	38	5	0.9
ABRL-4-2	s	11.3	5.58	9.4	2.2	25.9	0.5	6.6	2.2	5.4	0.9	6.2	460	163	799	6.6	49.7	1.05	52	12	2.1
ABRL-6-2	g	13.9	4.40	5.2	2.6	18.5	<0.3	4.5	0.6	4.07	0.94	6.8	8,380	859	11,000	23.8	91.5	3.94	88	136	49.5
ABRL-7-2	l	N.A.	6.90	6.8	6.4	4500	<8	800	600	800	114		4,630	11,900	88,900	51.7	4,750	32	1,860	801	52
ABRL-8-2	g	12.8	4.52	6.3	0.6	4.3	3.4	4.9	<0.2	0.66	0.63	6.3	268	40.6	30	7.9	47.0	0.25	33	11	7.9
AFC-1-2	g	13.4	4.11	4.6	0.9	3.2	0.7	3.4	<0.2	0.88	0.284	5.7	233	4.3	16	0.4	2.2	0.14	29	8	5.4
AFC-2-2	g	12.5	4.27	4.8	1.8	4	1.8	4	<0.2	0.61	0.404	7.4	183	12.2	22	1.0	14.7	0.36	118	7	1.0
ASC-1-2	g	13.2	4.62	4.4	1	12	0.3	3	0.6	1.05	0.321	6.7	119	2.7	11	1.1	6.1	0.11	47	15	0.4
ALC-1-2	s	11.5	4.62	4.5	1.2	3.2	<0.3	3.1	0.2	0.53	0.32	5.8	126	3.4	14	0.8	<0.5	0.17	101	28	0.3
ABRL-1-3	s	19.6	5.67	20.5	2.1	59.1	13.4	18.8	2.7	10.9	3.6	9.6	87	437	446	1.0	8.6	2.94	554	230	0.2
ABRL-2-3	g	14.2	4.68	6.8	1.0	13.6	1.7	6.5	0.35	1.4	0.63	19.8	3,190	63.0	2,060	22.2	36.3	3.02	29	8	6.5
ABRL-3-3	s	16.0	5.58	4.5	0.7	6.8	0.6	3.9	0.21	0.72	0.37	7.8	122	4.0	97	1.0	7.4	0.13	19	3	0.3
ABRL-6-3	g	14.2	3.80	4.9	1.9	18.1	0.5	4.9	0.31	4.2	1.2	11.4	551	614	137	4.2	14.6	2.63	97	48	3.4

Table 1 Chemical composition of waters and leachate for selected major and minor elements (continued)

Method Ref.		T °C	pH	Cl IC mg/L	SO₄²⁻ IC mg/L	HCO₃ POT mg/L	NO₃ IC mg/L	Na⁺ FP mg/L	K⁺ FP mg/L	Ca²⁺ FAA mg/L	Mg²⁺ FAA mg/L	SiO₂ MAS mg/L	Al ICP µg/L	Mn ICP µg/L	Fe ICP µg/L	Cu ICP µg/L	Zn ICP µg/L	As ICP µg/L	Br ICP µg/L	I ICP µg/L	Pb ICP µg/L
ABRL-7-3	l	N.A.	7.40	2200	112	676	<15	2400	1600	800	234		548	5,820	56,300	199	499	177	3,710	2,042	4.0
ABRL-8-3	g	14.6	4.14	6.7	0.9	5.5	2.4	5.2	0.19	0.95	0.6	9.1	131	57.0	154	3.1	21.7	0.33	62	32	0.8
AFC-1-3	g	13.8	4.15	4.8	0.8	5.4	2.1	4.3	0.21	0.71	0.46	9.4	213	19.0	31	1.0	12.5	0.47	73	30	0.4
AFC-2-3	g	13.0	4.26	4.9	0.6	6.8	1.6	4.6	0.22	0.72	0.44	10.8	60	11.0	11	0.3	4.8	0.32	29	5	0.2
ABRL-1-4	s	10.2	6.04	35	3.1	118	8.4	27	10	9.2	3.5	7.8	152	951	1,150	2.7	6.5	5.14	689	354	11.6
ABRL-2-4	g	13.9	4.22	11	1	19.4	1.4	11.4	0.34	1.8	0.87	21.7	137	14.6	116	13.4	18	2.29	20	14	2.5
ABRL-3-4	s	10.9	5.19	4.2	0.6	5.2	1.7	3.5	<0.1	0.52	0.38	7.4	147	6.9	91	3.0	9.7	0.09	13	2	1.6
ABRL-4-4	s	8.5	6.42	28	32	145	<0.3	22	9.6	41	4.1	5.9	2,380	1,840	3,790	117	127	4.27	123	37	57.4
ABRL-6-4	g	13.9	3.92	6.3	1.8	20.3	<0.3	4.3	0.24	6.5	0.84	8.4	682	1,340	238	7.1	21.7	1.91	105	77	24.6
ABRL-8-4	g	9.3	3.80	6.7	0.6	5.5	<0.3	5.1	0.11	0.93	0.65	7.9	206	198	6	1.8	3.6	0.24	44	9	1.4
ABRL-9-4	s	10.7	4.33	5.3	1.1	6.3	1.7	4	0.17	1.2	0.45	6.4	344	23.7	258	3.8	6.5	0.31	54	2	1.7
ABRL-10-4	s	10.6	4.78	5.4	0.8	4.5	2.4	4.2	0.11	0.63	0.47	7.1	88	2.5	36	0.4	1.0	0.06	18	<1	1.5
AFC-1-4	g	13.0	2.90	5.5	0.7	3.1	3.5	4.2	0.16	0.5	0.48	7.8	233	14.0	6	1.9	3.1	0.16	17	<1	0.4
AFC-2-4	g	12.5	3.32	5.6	0.5	6.1	3	4.8	0.2	0.74	0.55	9.2	256	34.1	59	1.1	1.7	0.61	25	2	1.3
ARIAM-1-4	s	10.6	4.50	6.6	2	8.1	5.2	4.6	0.83	1.9	0.7	7.6	578	33.9	422	3.4	10.2	0.43	42	7	9.0
ARIAM-2-4	s	10.5	5.44	6.9	2.4	10.9	5.5	4.8	1.5	2.3	0.85	8	175	29.0	113	2.2	8.5	0.32	45	7	4.5
ARIAM-3-4	s	10.6	5.22	6.3	2.3	8.2	5.6	4.2	1.3	2.2	0.8	7.5	179	17.2	99	1.2	2.1	0.19	27	2	0.7
ASC-1-4	g	13.9	3.87	3.9	0.6	4.8	1.2	3.3	0.13	0.72	0.3	8.2	94	3.2	8	1.4	5.7	0.12	13	<1	2.4
ALC-1-4	g	12.2	4.12	4.8	1	5.6	0.6	3.9	0.13	0.66	0.4	8.2	77	14.0	39	4.4	14.9	0.16	15	2	10.0
ABRL-1-5	s	11.7	5.57	64	13	111	29	45	15	11.1	4.0	7.2	217	489	397	2.8	7.2	2.85	487	141	0.16
ABRL-2-5	g	14.1	4.22	6.9	0.8	23.5	<0.3	8.9	0.37	2.5	1.4	21.7	68	284	246	7.3	12.8	2.45	38	72	0.76
ABRL-3-5	s	10.3	4.69	4.5	0.6	5.5	1.5	3.8	0.12	0.72	0.46	9.6	247	3.2	167	0.6	1.1	0.09	15	2	0.05
ABRL-6-5	g	14.4	4.34	5.6	2.5	24.1	0.3	5.5	0.26	5.4	0.68	16.1	551	700	240	2.8	9.5	1.9	58	31	0.62
ABRL-8-5	g	12.3	4.19	7.2	2.1	10.2	2.7	5.9	0.2	2.1	1.1	11.1	90	78.8	81	9.0	47.6	1.12	58	2	0.84
ABRL-10-5	s	12.5	5.35	7.8	1.1	5.4	6.3	6.3	0.2	1.1	0.89	7.7	126	82.5	43	0.8	<0.5	0.06	53	<1	<0.01
AFC-1-5	g	13.8	3.35	4.9	1.2	3.1	2.8	3.8	0.21	0.36	0.54	7.2	240	14.0	<10	0.5	0.7	030	20	<1	<0.01

Table 1   Chemical composition of waters and leachate for selected major and minor elements (continued)

Ref.		T	pH	Cl⁻	SO₄²⁻	HCO₃⁻	NO₃⁻	Na⁺	K⁺	Ca²⁺	Mg²⁺	SiO₂	Al	Mn	Fe	Cu	Zn	As	Br	I	Pb
Method				IC	IC	POT	IC	FP	FP	FAA	FAA	MAS	ICP	ICP	ICP	ICP	ICP	ICP	ICP	ICP	ICP
		°C		mg/L	mg/L	mg/L	mg/L	mg/L	mg/L	mg/L	mg/L	mg/L	µg/L	µg/L	µg/L	µg/L	µg/L	µg/L	µg/L	µg/L	µg/L
AFC-2-5	g	14.2	4.02	5.1	0.6	7.8	2.4	4.8	0.18	2.6	0.52	10.9	263	14.2	<10	0.5	<0.5	0.31	19	<1	<0.01
ARIAM-1-5	s	12.0	4.41	9.8	3.3	4.1	17	7.7	1.9	3.6	1.4	8.6	63	10.2	25	0.8	0.5	0.11	53	<1	<0.01
ARIAM-2-5	s	11.8	4.85	9.8	2.8	8.6	16	7.2	1.5	3.6	1.7	9.2	94	27.1	57	1.5	1.1	0.27	56	2	0.02
ARIAM-3-5	s	12.0	4.72	8	2.4	5.8	15	5.5	0.97	3.2	1.6	9.2	73	16.3	36	1.6	0.8	0.17	40	<1	0.01
ASC-1-5	g	14.8	4.26	3.7	0.8	4.9	0.9	3.2	0.12	0.8	0.46	8.1	85	2.0	<10	0.9	<0.5	0.08	12	<1	<0.01
ALC-1-5	g	12.3	5.05	4.8	1.2	8.5	<0.3	3.9	0.31	2.2	0.57	9.6	2,650	29.6	1,130	1.5	2.8	1.82	18	2	0.72
ABRL-1-6	s			48	2.9	14.2	1.5	7.6	0.5	1.43	0.74		952	979		0.8	19.9	1.33	516	32	0.1
ABRL-2-6	g			8.9	1.9	20.9	<0.3	8	0.35	2.7	1.3		101	1,900		4.2	12.8	2.19	153	143	1.3
ABRL-3-6	s			4.3	0.4	5.5	1.3	3.7	<0.1	0.66	0.39		205	4.3		<0.2	3.6	0.13	14	4	<0.01
ABRL-6-6	g			6.0	1.7	46.2	<0.3	6.5	0.29	10.2	1.2		551	962		2.3	14.7	4.72	65	25	1.3
ABRL-8-6	g			6.9	1.6	12.3	3.5	6.2	0.21	2.5	1.2		116	81.4		1.8	13.8	1.30	71	4	0.6
AFC-1-6	g			5.0	1.2	5.4	1.1	4.2	0.16	0.73	0.5		145	13.3		<0.2	3.2	0.43	18	1	<0.01
AFC-2-6	g			5.9	0.5	8.2	2.6	5.3	0.16	1.2	0.54		131	30.3		0.2	6.3	0.65	44	2	<0.01

The s, g, and l, indicate surface water, ground water, and leachate respectively. The last digit of each sample reference indicates sampling campaign. pH was measured in the field except for the leachate (ABRL-7 samples) which was measured in the laboratory. Methods of analysis as follows – IC: Ionic Chromatography; POT: Potentiometry; FP: Flame Photometry; FAA: Flame Atomic Absorption Spectrophotometry; MAS: Molecular Absorption Spectrophotometry; ICP: Inductively Coupled Plasma – Mass Spectrometry.

3.3 Water geochemistry

Chemical analytical data obtained in ground and surface waters around and beneath the facility are presented in Table 1.

No wells exist on the waste disposal facility ridge, except for two monitoring bore-holes located inside the facility fence and several water wells drilled in its immediate north neighbourhood for water supply to the facility itself (Figure 2). Direct sampling of underground waters far from the facility must therefore rely on a few springs that can be found on the ridge southern flank and on some water collection works (mainly underground pipes) that concentrate shallow (?) underground waters to small overflowing reservoirs. These waters are chemically fairly homogeneous, having constant temperature (around 14ºC) all year round, low conductivity (27–35 μS/cm), fairly low pH (around 4.5 or less), Eh values between 370 mV and 440 mV, and low total ionic concentration.

The creeks draining the ridge, most of them ephemeral or at most semi-permanent, are very short and their waters are very similar to underground waters, except that their temperature is slightly warmer and more variable, and pH values are consistently higher, in the range 5.2–5.6.

Surface contaminated waters, i.e., creek waters originating inside the facility fence, have the highest pH values (above 6) and most of them show visual signs of pollution. The permanent creek that drains the notch wherein the facility was built (samples ABRL-1) displayed initially a fluffy bright orange deposit covering everything underwater and turning black upon desiccation; the water was partially covered by thin oily films imparting a greyish colour to the surface, but nevertheless the creek was able to support apparently healthy plant and animal life. In later times, all this had disappeared along with most of the biological community once present. Rill water escaping from the north fence wall of the facility has a light brown colour, and upon evaporation in pools, its load of organic contaminants becomes evident. The ephemeral character of this run-off prevented representative sampling of the running water, but stagnant or quasi-stagnant pool water has been as regularly sampled as weather allowed.

In the immediate neighbourhood of the facility, underground waters are chemically different from the waters collected outside the zone that may reasonably be supposed to have been affected by the facility operation, the concentrations of almost all analysed elements being significantly higher than background.

From Table 1, it can be seen that the underground water geochemical background has remained constant, despite the non-steady-state of the hydrogeological conditions prevailing during most of the sampling period. The same is not true of the chemical composition of waters affected by the facility operation. Series ABRL-1 displays ever increasing concentrations of both major and minor elements and most of the ground waters collected around the facility reveal a general slow increase in metal concentrations, contrasting with the lack of any discernible trend in the background waters. This suggests that the facility has created a halo of slight groundwater contamination, which is gradually intensifying; regretfully, the spatial distribution of springs and water wells, mostly located on the south slope of the ridge, is not dense enough to allow an eventual simultaneous spreading of this halo to be observed.

The creek where the ABRL-1 samples were collected drains to an important perennial stream, which differs chemically from the regional undergroundwater geochemical background, because its watershed lies partially outside the local granite massif and

because it is affected by human activities (mostly agriculture) not present on the facility ridge. This stream has been sampled upstream and downstream of the ABRL-1 creek confluence (samples ARIAM) to determine the latter's chemical influence on the stream. Table 1 shows that at the point of confluence (ARIAM-2), the concentrations of many chemical elements rise significantly and then decrease slightly downstream, presumably due to fixation on organic matter or living organisms since the stream velocity is quite high and there are no sediments available to act as metal sinks. This downstream trend is, however, not very intense and can easily be obliterated by other geochemical signals (most likely due to agricultural activities in the stream watershed), as happened at the moment of sampling survey #5.

Considering the concentrations of Cl^-, HCO_3^-, and SO_4^{2-}, it is possible to see that all uncontaminated waters form a tightly knit cloud separated from all other water samples (Figure 3). On the other hand, contaminated surface waters form a well-defined trend which, if backward and forward extrapolated, passes through the borehole water and leachate data points, thus suggesting that these three sample groups define a single mixing line (Figure 3(A)). If only chloride and sulphate concentrations are taken into account (Figure 3(B)), this single mixing line incorporates all the samples and is thus the line that denotes the progressive contamination of the natural waters with the leachate.

Figure 3   Major anion concentration plots of water samples beneath and around the waste disposal facility. Crosses and circles represent samples of surface and ground waters (respectively) located away from the facility and taken to be uncontaminated. Squares correspond to ground waters collected in boreholes located inside and not very far from the facility fence, which may be contaminated. Diamonds represent surface water samples emanating from the facility, showing visual signs of pollution. Triangles represent leachate samples. In A, the dashed line corresponds to the forward and backward extrapolation of the linear relationship obtained with the contaminated surface samples; in B, the grey circles are the average points of each group of water samples
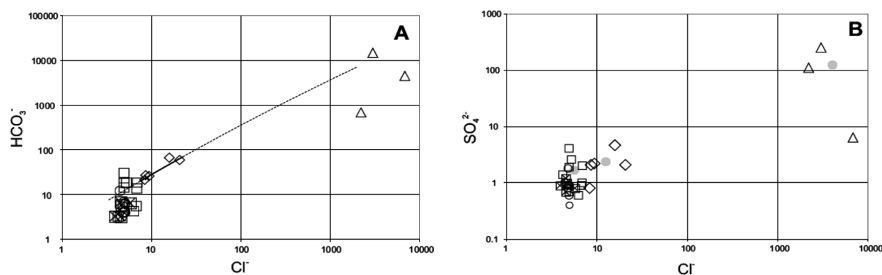
Considering now all the major elements, the chemical load induced by the facility (defined as each element concentration in the sample divided by the average concentration of the same element in background waters, averaged for all elements) is always at least 1.7 in the affected waters, but may be as high as 12.5 in the rill waters draining to the north, and has average values around 3.4 in most of the surface and underground waters directly concerned by the facility. The same pattern emerges when the trace element concentrations are considered: chemical loads (defined as above) are now much higher (average values within the facility fence are around 23, but reach 53.9 in one of the monitoring wells) because of the diminutive background values of most of the trace elements, and there is a clear difference between underground and surface

waters, the former having higher chemical loads. Underground and surface waters also differ chemically: whereas underground waters are mainly loaded with transition and heavy metals, surface waters are especially enriched in alkali and alkali-earth metals and in halogens.

Overall, chemical loads of surface waters are always much lower than those of underground waters, the only exception being the permanent creek emanating from the south fence wall of the facility, which, in the first sampling campaign, showed a chemical load of the same magnitude as the most polluted monitoring well (sample ABRL-6). Since this creek does not percolate the waste piles, its chemical load must be explained by its tapping of underground heavily contaminated waters.

Saturation indices of selected mineral phases in the analysed waters were calculated with PHREEQC (Parkhurst and Appelo, 1999) (Figure 4); groundwaters are predominantly undersaturated relative to most phases. This is coherent with the observation that nearly all fractures are open and devoid of any mineral fillings. The only secondary mineral phases that may be oversaturated are kaolinite and gibbsite; kaolinite is widespread as a result of extreme weathering of feldspars and X-ray diffraction results of the weathering products do not exclude the presence of gibbsite (Table 2). Higher pH and chemical concentrations allow a greater number of phases to be supersaturated in the contaminated waters and landfill leachate. One of them, barite, is indeed found in the sediments laid down by surface waters having percolated the waste pile, which are frequently saturated (and sometimes slightly supersaturated) in this mineral.

Figure 4 Saturation indexes vs. pH of the sampled waters collected in the first (A) and second (B) campaigns corresponding to a summer and winter period, respectively (see online version for colours)
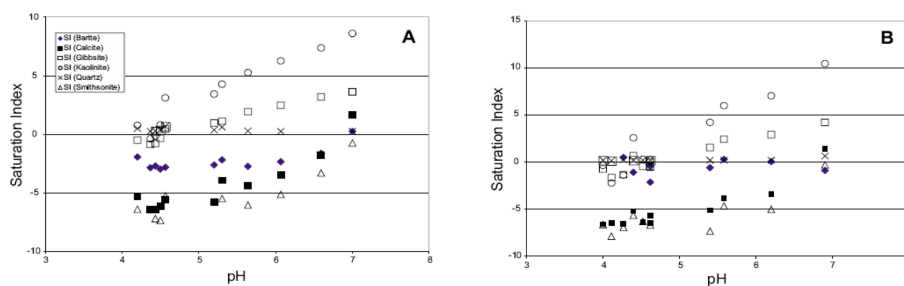
Table 2 Partial chemical analysis of soils. Sample reference T correspond to the top soil (B horizon) and B to the corresponding base soil (C horizon)

Sample	Cu ppm	Mn ppm	Ni ppm	Pb ppm	Zn ppm	Al %	V ppm	As ppm	Ba ppm	Br ppm	Cr ppm
LC 4-1	5	296	2	32	85	12.17	26	3	620	84.5	13
LC 4-2	7	236	2	38	90	13.08	29	2.4	600	42.8	13
LC-6B	4	236	2	36	77	14.52	23	3.5	490	54	10
LC-6T	10	144	2	34	68	6.41	21	2.7	450	40.2	11
LC-7B	21	328	5	41	123	13.11	28	5.2	540	80.3	13
LC-7T	40	242	3	32	66	10.99	26	5	340	72.7	14
BRL-1B	6	196	3	37	57	7.23	26	4.8	470	73.6	12
BRL-1T	16	291	5	41	75	10.53	30	8.3	310	96.5	13

Table 2   Partial chemical analysis of soils. Sample reference T correspond to the top soil
(B horizon) and B to the corresponding base soil (C horizon) (continued)

	Cu	*Mn*	*Ni*	*Pb*	*Zn*	*Al*	*V*	*As*	*Ba*	*Br*	*Cr*
Sample	ppm	ppm	ppm	ppm	ppm	%	ppm	ppm	ppm	ppm	ppm
BRL-2B	6	287	6	34	67	4.79	33	4.8	600	42.3	14
BRL-3	7	238	5	41	72	7.98	34	7.1	410	79.8	15
BRL-4B	6	258	2	35	68	11.74	28	5.9	480	62.4	17
BRL-6B	4	406	5	36	73	10.02	30	6	500	62.6	12
BRL-7	17	377	4	35	77	11.60	26	8.5	380	99.6	13
BRL-15	11	199	3	48	52	8.69	21	7.4	410	202	11

3.4   *Mineral substrate geochemistry*

As is the case with background waters, soils are almost invariant chemically. They are
thin, lack maturity, and are chemically similar to altered granite (Table 3). This is also the
case with the sediments laid down by the small creeks and rivulets draining the facility
ridge (Table 4). A list of the identified minerals in the different sampled materials
is provided in Table 2. In the case of soils and altered granites, there is no difference in
the chemical composition between samples in the immediate vicinity of the facility and
samples collected at other places, even when trace elements are considered; thus, there is
no diffuse, airborne or otherwise, dispersal of pollutants emanating from the facility.
The same is not true, however, of creek sediments. Creeks draining northwards parts
of the facility enclosure, including the waste piles themselves, lay down sediments that
have higher than background metal concentrations and that display, for those elements,
negative downstream concentration gradients. The most important contaminant metals
are Cu, Zn, Cr, Ni and Pb. At the fence, Cu concentrations are two orders of magnitude
above background and decrease downstream 4- to 18-fold, depending on the stream
considered. Maximum Zn concentrations at the fence are an order of magnitude above
background levels, but its downstream gradients are shallower, final concentrations in the
region surveyed being 2–5 times above background. Analytical electron microscopy
techniques indicate that Cu, and to a lesser extent Zn, are found as detrital brass particles
and as surface coatings on natural mineral grains, and that autigenic phases, such as barite
and sphalerite, are being formed in the sediments (Gonçalves et al., 2002, 2004). μ-PIXE
examination of the samples (Gonçalves et al., 2002) has confirmed and detailed these
observations by showing that, apart from the autigenic minerals just mentioned, iron
hydroxides are also being formed in the sediments and that the most concentrated
contaminant metals occur entirely (or partially in the case of zinc) as adsorbed films on
the mineral surfaces. This adsorption is independent of mineral species and seems to
be due to complexation of the metals by organic films coating the mineral grains,
since sequential extraction results have shown that significant amounts (up to 70%
of the total contents of copper, for example) of the metals contained in the sediments
are complexed by organic molecules; this is especially the case of Cu, Zn and Pb
(Gonçalves et al., 2004). The other elements mentioned above have distributions similar
to those of Cu, Zn and Pb, but with lower maximum concentration anomalies and
shallower downstream gradients. The sediments laid down by these creeks contain many
other elements in concentrations above background levels, but the values observed are
too similar to background to allow a statistical certitude of their origin in the facility.

However, elements such as Mg, Ba, Cs, and Fe do display negative downstream concentration gradients, and several others have their maximum concentrations at the fence wall, although no discernable downstream trend can be observed in their concentrations.

Table 3 Chemical analysis of the creek sediments for major elements and selected minor elements. A representative granite sample analysis (PP-1) is also given at the end of the table

Sample*	SiO_2	Al_2O_3	Fe_2O_3	MnO	MgO	CaO	Na_2O	K_2O	TiO_2	P_2O_5	LOI**	Ba	As	Y	Cu	Zn	Pb	Ni	V
BRL-2T	73.56	12.43	2.16	0.040	0.59	0.37	1.22	4.48	0.514	0.16	4.94	617	7	11	6	61	39	3	26
BRL-4T	56.81	17.16	3.20	0.057	0.89	0.66	1.74	4.62	0.522	0.25	12.97	610	10	16	33	118	41	7	42
BRL-6T	76.39	11.18	1.91	0.031	0.50	0.41	1.28	4.45	0.345	0.18	3.84	603	6	9	25	75	30	3	19
BRL-9 FA	60.41	19.16	4.08	0.071	1.05	2.07	2.37	4.73	0.943	0.55	3.82	789	15	54	1016	852	117	34	52
BRL-10 FA	35.81	23.86	6.62	0.076	1.50	1.02	0.52	2.88	0.758	0.56	25.12	484	58	36	478	785	125	22	79
BRL-11 FA	46.84	20.39	4.73	0.073	1.20	1.19	1.75	4.32	0.729	0.45	16.86	644	18	33	258	455	86	21	59
BRL-12 FA	48.29	21.00	4.84	0.082	1.16	1.27	1.76	4.08	0.798	0.52	16.36	625	19	39	262	449	83	23	65
BRL-13 FA	44.58	21.99	4.52	0.056	1.15	0.74	1.43	3.94	0.678	0.30	19.25	513	21	27	55	162	45	9	50
BRL-14 FA	42.57	24.51	3.62	0.041	0.89	0.44	1.24	3.23	0.470	0.33	21.66	365	31	29	42	126	46	4	34
BRL-16 FA	44.71	23.87	4.68	0.055	1.15	0.82	1.40	3.97	0.687	0.38	18.54	531	23	33	100	199	49	10	56
BRL-9 FS	63.35	16.16	3.30	0.048	0.95	1.67	2.21	4.98	0.642	0.36	4.88	740	11	23	591	485	66	21	36
BRL-10 FS	34.87	23.58	6.66	0.076	1.54	1.04	0.57	2.81	0.761	0.58	26.65	440	61	36	427	692	121	21	75
BRL-11 FS	53.86	18.56	4.19	0.065	1.13	1.03	2.01	4.91	0.660	0.32	12.02	617	13	20	163	313	57	14	47
BRL-12 FS	54.00	18.55	4.22	0.084	1.08	1.25	1.99	4.51	0.929	0.43	12.65	620	16	29	206	324	63	16	52
BRL-13 FS	43.84	21.59	5.69	0.075	1.74	0.70	1.40	4.26	0.811	0.26	18.55	523	17	22	56	195	39	12	71
BRL-14 FS	42.53	25.07	4.08	0.041	1.00	0.42	1.21	3.48	0.496	0.34	21.39	331	32	27	33	106	38	5	39
BRL-16 FS	43.38	23.09	5.29	0.066	1.57	0.76	1.33	4.04	0.760	0.31	18.17	542	20	26	90	198	46	11	65
PP-1	70.02	15.38	2.95	0.046	1.02	1.50	3.13	4.41	0.533	0.26	0.85	636	1	14	3	99	27	5	42

*Major oxides and LOI in %, minor elements in ppm.

**LOI: Loss On Ignition.

Table 4   Mineralogy present in the different sampled material

Mineralogy	Granite	Soils	Fractures	Contaminated sediments
Quartz	*	*	*	*
Feldspar	*	*	*	*
Muscovite	*	*	*	*
Biotite	*	*		*
Chlorite	*	*		*
Illite		*	*	*
Illite-Smect. (IS)				*
Kaolinite		*	*	*
Ilmenite	*			*
Monazite	*			*
Barite				*
Sulphides (sph, py, cpy(?))				*
Gibbsite (?)			*	
Artificial alloys				
Fe/Ti/Cr				*
Cu/Zn				*
Fe pellets				*

4   Geophysics

Geophysical surveys, using resistivity methods, were carried out at four different times, June 2000 (Mota et al., 2004), February 2001, June 2004 and May 2006, to monitor the environmental evolution around the facility. Three profiles were set up with an E–W orientation, using Wenner array (profiles I, II and III in Figures 1 and 5). The 360 m long profile I (3 m of electrode spacing) was carried out at about 150 m north of the dump cell. Profile II (with a total length of 300 m – 3 m of electrode spacing) was performed close to the southern limit of the dump cell and profile III (also 300 m long, but with 4 m electrode spacing) was carried out about 350 m south of the dump cell. Local topography and suspected main fault orientation, within the landfill, constrained the E–W orientation of these profiles.

Figure 5   Monthly precipitation in the monitoring years. See text for details. The line marked landfill is data collected at the facility location
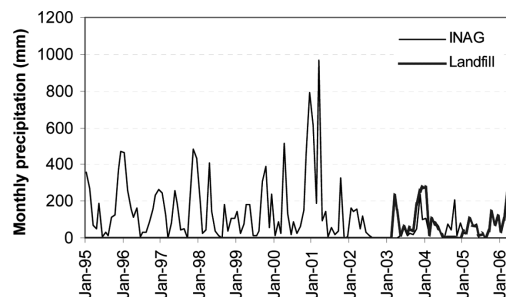
These surveys were supplemented with a VLF-EM survey carried out in the vicinity of the landfill in the 2004 summer (Monteiro Santos et al., 2006). The VLF data was collected in 12 profiles, oriented roughly E–W, with measurements at 8 m intervals, using a frequency of 19.6 kHz. Fraser filtering (Fraser, 1969) was used for a qualitative interpretation of the data. This method transforms the zero-crossing points into peaks, thus enhancing eventual conductive structures. The centre of the anomalous structures should be located directly beneath the peaks of the filtered data. The latter were presented in Monteiro Santos et al. (2006) as profiles, and are now interpolated and presented as a map (Figure 6).

Figure 6   Resistivity models for profiles I to III, for June 2000, February 2001, June 2004 and May 2006, obtained with RES2DINV. Low resistivity zones marked A and B are also marked in the VLF map (Figure 8)
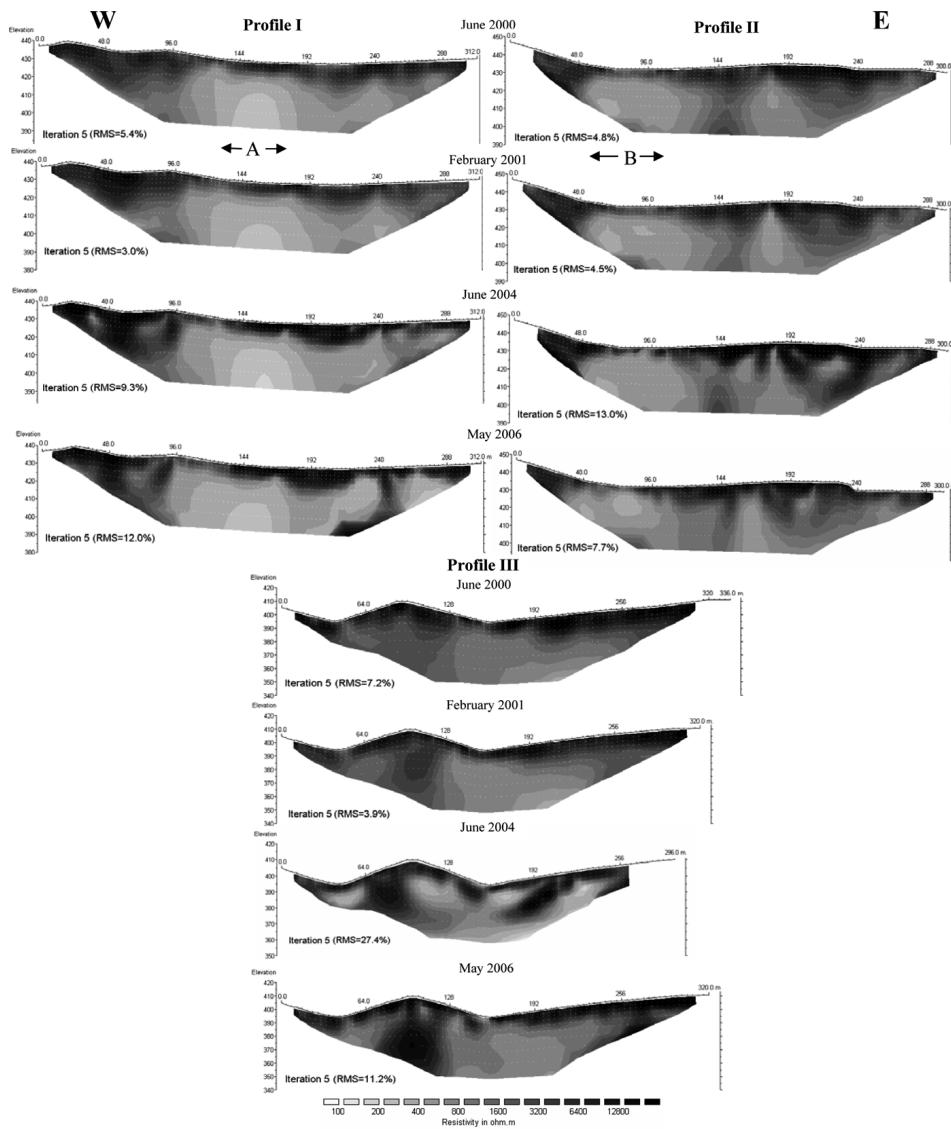
4.1   Geophysical results

The weather conditions were highly variable during the six-years period of the monitoring work. The annual evolution of the precipitation is shown in Figure 7. Data for the period January 1995 to January 2006 is an average of data collected in two INAG (National Water Institute) meteorological stations located to either side of the landfill facility. Meteorological data were collected from March 2003 to April 2006 at the facility location. Figure 7 shows that the 2001 survey was performed under exceptional rainfall conditions leading to high leachate production and to high water content in the terrain. These conditions were reflected in the fieldwork. During dry periods, the contact resistance was high, especially in profiles II and III, giving high measurement errors. Besides, between 2001 and 2004, a significant land movement took place at profile III location, with deposition of up to 2 m of residual soil. Despite all efforts to lower the contact resistance, it was impossible to have good data at this location in the 2004 survey. Even discarding the eastern part of this profile, these difficulties are reflected in the high RMS of the final model for profile III, obtained from the 2004 survey. In 2006, there was also a topographic change around coordinates 240 of profile II, in this case with loss of land.

Figure 7   Relation between the precipitation occurred two month before each survey and the resistivity ratio (calculated at the coordinate 164, profile I) at the levels 426 m asl (immediately beneath the surface) and 412 m asl (in the low resistivity anomaly)
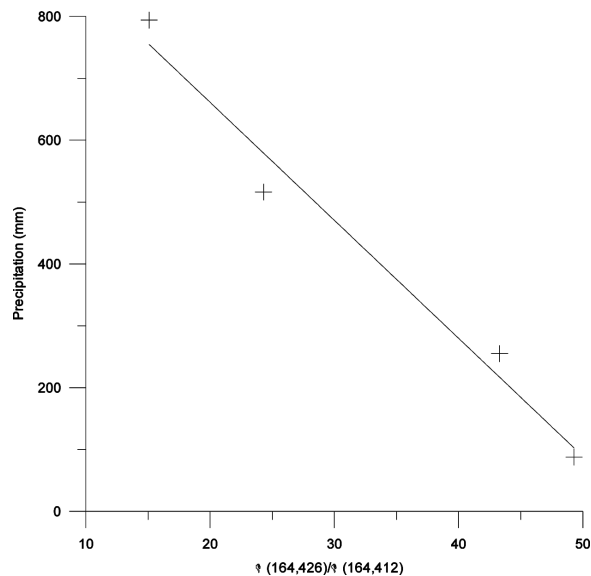
The resistivity models for each profile, calculated with the Res2Dinv program (Loke and Barker, 1996), are shown in Figure 5. To evaluate the relation between the precipitation and the evolution of the main resistivity anomaly, the total rainfall occurred in the two months preceding each survey was plotted against the resistivity ratio between two points at two different depths inside the low resistivity anomaly detected in profile I. The results, shown in Figure 8, indicate that the anomaly intensifies relative to background under dry conditions and is diluted in wet periods.

In all resistivity models, the overburden resistivity is generally above 6400 ohm-m with a maximum thickness of 5 m, which is thought to express the dry conditions prevailing in the first few metres of the granite massif. In contrast, the basement usually presents a lower resistivity of 1600 ohm-m, thought to reflect wet conditions in depth. Apart from this surface-depth contrast, all profiles are dominated by the presence of a deep-lying low resistivity anomaly in their central-western zone. High resistivity deep domains, most prominently the one seen at the western tip of profile II, coincide with unfractured (and thus, unaltered and dry) granite domains, as shown by the geological survey.

Figure 8 Contours of the Fraser filtering results. Positive anomalies marked A and B are also marked in resistivity models (Figure 5)
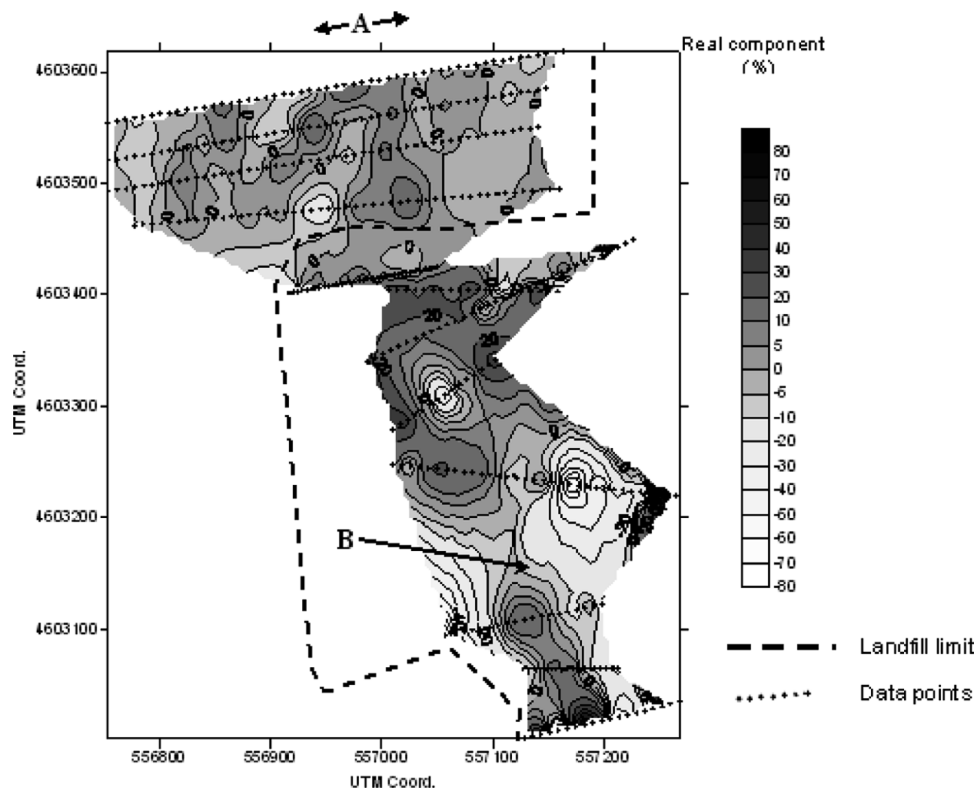
The character of the anomaly varies from profile to profile. In profile I, the resistivity falls to very low values (<280 ohm m), and the anomalous zone is clearly not confined in depth. In profile III, the anomaly, although clearly recognisable, has central resistivity values barely below those of the geophysical background. The anomaly is thus very intense and deep under profile I and, although more circumscribed in profile II, has a lower intensity in profiles II and III.

In the latter profiles, the anomaly is located beneath the thalweg whereto leachate collects under the waste piles. In profile I, the anomaly is slightly to the west of the fracture zone originating the thalweg just referred to, but coincides with a NNW-SSE fracture zone, detected in the geological field work. As the examination of the eastern

parts of the profiles makes clear, fracture zones do show up as low resistivity anomalies, but there is no geological reason whatever why the fracture zones coinciding with the main resistivity anomaly should have significantly higher fracture density or water contents and hence a lower electrical resistivity than any other vertical fracture zone affecting the massif. Regions of positive anomaly in the VLF-EM map also indicate the presence of subsurface conductive domains. Those marked with A and B in the VLF map (Figure 6) are well correlated with the low resistivity anomalies in resistivity profiles I and II (Figure 5), thus confirming the anomalous character of the fracture zones just referred to. In the absence of a plausible geological cause, the most parsimonious explanation for the low resistivity anomaly is the presence of waste leachate originating in the landfill.

The general low resistivity domain shown in the three profiles is a permanent feature. However, changes in its intensity and size were recorded during the monitoring programme. In normal conditions – in the absence of a contaminated plume – resistivity variations would result from increased water circulation associated with precipitation, and this is observed in the lesser anomalies beneath coordinate 170 in profile II and beneath coordinate 270 in profile I. On the contrary, Figure 8 shows that the main low resistivity anomaly in profile I intensifies relative to the surface under dry conditions. This seems to reflect a lower dilution of the leachate, due to lower groundwater volumes available under dry conditions, because a significant amount of groundwater drains rapidly out of the granite massif through its conspicuous and abundant open fractures.

5 Discussion

The waste disposal facility under study has been built in a lithologically very homogeneous area. The steep relief and chemical nature of the bedrock ensure that weathering is almost isochemical and that soils do not differ significantly, apart from their much higher organic matter content, from the weathered bedrock. This means that it is fairly straightforward to establish the chemical background of the locality and that any deviation induced by human activities can be easily detected, at ppm levels for many elements.

The facility has been operating for eight years and its chemical impact on the environment, although hardly felt at all in the field, is already discernible. So far, there is no detectable diffuse surface flow of chemical elements (carried by winds, or some other means) emanating from the facility, since all soils, even those adjoining its fence, have background chemical compositions. However, concentrated outflow of surface run-off waters is carrying away a wide range of elements, which are being fixed to a small extent in the sediments deposited in creek beds.

There is no indication whatever of pervasive underground outflow of material from the facility, since altered and unaltered bedrock analyses fail to show the facility to be immersed in a halo of rocks showing signs of chemical contamination. However, the chemical signature of the very slightly contaminated waters, and the different composition of underground and surface waters, may be taken as an indication that various chemical elements are being injected into the natural waters and being transported at different speeds, the slowest ones residing still for a great part underground and the swiftest ones having already a strong presence in surface waters. The reason for the differential interaction of the chemical elements with the geological basement is at

present still uncertain in its details, but a likely candidate mechanism for the difference is chemical complexation of the transition and heavy metals by organic ligands (with special emphasis on the organic acids), which, because of their abundant functional sites able to interact with mineral surface charges, would lag behind soluble and non-interacting aqueous-complexes (Gonçalves et al., 2004).

Leachate, surface-contaminated waters, borehole waters and uncontaminated waters seem to form a single mixing line in the $SO_4^{2-} - Cl^-$ plot. In the $HCO_3^- - Cl^-$ plot, however, the mixing line joins leachate and borehole waters and passes distinctly above the cloud of points representing uncontaminated waters. This apparent deviation concerning HCO_3^- is interpreted as a result of the highly acidic and extremely oxidising chemical environment of the natural groundwater, which would promote the oxidation of the organic compounds injected from the facility, producing an excess of this anion. Because this is a young system and is far from steady state, there seems to be some seasonal variation in the water chemistry, especially for those samples showing signs of contamination. However, successive ABRL-1 samples plot ever nearer to the leachate samples in both plots, a tendency that is also observed in all waters most affected by the presence of the facility.

Waste stabilisation may lead to calcite and other carbonate phases precipitation (Manning, 2001), but our calculations with PHREEQC indicate that only the leachate waters are supersaturated in carbonates; this indication must however be taken with care, because the high salinity of the leachate reduces the calculations reliability, which assumed the usual model for dilute solutions with simple electrolytes. It is not known if carbonate precipitation has begun inside the waste piles, but no carbonates are found in the analysed samples, not even in the sediments, where they could have acted as sinks for the most important metals analysed.

According to the available data, there is ample evidence for concentrated flow of leachates to the outside of the facility. The permanent creek emanating from the south fence wall of the facility (samples ABRL-1) has a chemical load of the same magnitude of the most contaminated monitoring well (samples ABRL-6). Since this creek does not percolate the waste piles, its chemical load must be explained by its tapping of underground heavily contaminated waters. However, this creek water entirely lacks any significant amount of the organic compounds identified by Solid Phase Extraction Gas Chromatography (SPE-GC-MSD) in the leachate, samples ABRL-7, and in the contaminated sediments (Gonçalves et al., 2004). Retention in the granitic massif prior to upwelling is not a viable explanation for this, because flow conditions and the geological setting do not seem to foster high retardation factors for these organic compounds. Even considering that apolar and weakly monopolar organic compounds are likely to have higher adsorption coefficients onto inorganic surfaces (Schwartzenbach et al., 2003), at least low molecular weight aliphatic carboxylic acids should have been detected as they have been shown to be the major landfill leachate constituents, presently still in its acidic stage (Gonçalves et al., 2004; Pohland and Kim, 2000). The general absence of organic compounds in this creek water seems thus to indicate that, in the present stage of the system development, the oxidation process previously mentioned while discussing the high HCO_3^- contents of the borehole waters, essentially goes to completion. Further monitoring should confirm or infirm this interpretation.

Given the homogeneous character of the granite massif, the low resistivity anomaly seen in the geo-electric profiles must be assigned a non-geological origin, most probably a plume of leachate entrained in the natural groundwater circulation. Inspection of the

resistivity profiles and of Figure 6, together with Karous–Hjelt filtering of the VLF-EM data (Monteiro Santos et al., 2006), shows that this plume follows the fracture zone whose erosion has created the topographic notch wherein the facility was built. The geophysical data resolution (intrinsic or caused by constraints in profile location) precludes the exact location of the leak, although there are faint indications that it may be in the central leachate collection works of the facility. Most of the anomaly extends northwards from this inferred leaking point, and in the northernmost resistivity profile it appears unconstrained in depth, in sharp contrast to its lesser intensity and stronger depth confinement to the south. This seems to indicate that most of the plume flows to the north as expected from the hydraulic heads established by the regional topography, the valley to the north of the ridge being several hundred metres deeper than the valley to the south. However, some southwards flow of the plume does exist, as shown by the ABRL-1 water samples collected at the facility south fence.

From the data available and discussed above, it is possible to infer that leachate injection to the environment is being done at two different points:

- through a leak concealed under the facility itself

- through the north fence wall, where surface run-off having percolated the waste piles and several dependences of the facility, is allowed to escape freely to the surrounding countryside.

The underground leak gives rise to an obvious conductive anomaly, reflecting underground circulation of contaminated waters, which wells up to the south forming a clearly polluted water creek, and spreads underground to the north, leaving its chemical signature in all springs and water wells available. The surface leak is resulting in the deposition of metals in superficial sediments at distances that already reach 200–300 m from the fence wall. Both leaks transport a very diverse set of chemical elements, which differ from one another in their ability to interact with the geological substrate and with the organic matter that comes along from the waste piles or is met with upon contact with the biosphere. This has already resulted in a visible difference in the chemical composition of the underground waters, when compared with surface waters, and in the fact that not all elements carried dissolved in waters find their way to a fixed state in sediments.

It is worth noting that the underground injection of leachate does not translate in a spherical domain of heavy pollution. This is due both to dilution by abundant groundwater (at least under normal rainfall conditions) and to very rapid groundwater recharge and discharge through the ubiquitous open fractures of the granite massif. Thus, although the continuing injection of leachate will progressively deteriorate groundwater conditions, it is expected that the contamination indicators will worsen slowly, as observed, since most of the contaminants will be swiftly exported to great distances through flushing of underground water circulating in the massif fractures. This effect of dilution and rapid export to great distances inferred to exist underground is also well observed at the surface in the case of the river receiving ABRL-1 creek waters: although these are the most contaminated surface waters, they induce a minimum (yet detectable) chemical anomaly in the river, which fades partially downstream, due to the larger volume of the stream waters and the speed of its current. Note, however, that the underground dilution effect will be effective only as far as the leachate plume can remain focussed by the fracture zone. Far from the facility, this will not be possible and

huge amount of contaminants may pollute huge volumes of granite before its deleterious effects are felt.

It should be stressed that, in all cases, the levels of contamination observed are still extremely low, and do not qualify as pollution by any standard available. All of them are, nevertheless, clear deviations from background and are worsening with time. This is cause for concern, because although the surface flows of chemicals can be easily recaptured and treated in conventional ways, the same is not true of the disperse underground flow that geophysical data show to the north of the facility. In this case, huge amounts of pollutants will have contaminated huge amounts of rock massif before springs and wells scattered over a large area in the long hill slope that extends from the ridge to a major heavily populated valley floor will start to deliver degraded water. There seems to be no scientific or engineering solution to the mitigation of such a situation.

The data obtained also allow some thoughts on the long-term natural attenuation of this system. Natural waters circulating in the granite massif are fairly acidic and the soils resulting from its weathering have also a fairly low pH. This means that cations eventually introduced in the soils will be for the most part remobilised during rainy periods and that their underground fixation is also unlikely, not only because of the underground waters acidity but also because of their very low total mineralisation, which makes them undersaturated in most of the common supergene mineral phases.

Once introduced in the underground circulation, cations are most likely to be quickly exported to fairly great distances due to the general high fracturing of the granite and the open character of its fractures. Retention by adsorption on mineral surfaces cannot be expected to occur at relevant rates and retention by adsorption or complexation by low mobility organic compounds is being hampered by their destruction due to the oxidant conditions prevailing underground.

Surface sediment pollution can be very easily suppressed by simple engineering works, but underground pollution is most likely to continue unabated, leading to an expanding halo of contaminated water points, whose composition may shift in the long run from metal dominated to organics (plus metals?) dominated, if the underground input of organic compounds becomes high enough to suppress the oxidation capacity of the natural geological system.

6   Conclusions

An array of comparatively low-cost monitoring techniques was used to characterise the environmental impact around a young landfill facility located on top of a fractured granite massif. Data obtained give an accurate picture of the situation, enabling the detection of a latent hazardous situation.

The general picture is that of a very faint halo of dispersed chemical elements, transported mainly by underground waters inside a fracture zone, and of slight base metal contamination in sediments laid down by surface run-off waters escaping from within the facility and draining operational pavements and the waste piles themselves. This picture is slowly worsening due to continuing injection of contaminant fluids in a context of strong underground dilution and rapid circulation of groundwater.

The geochemical signature of these very slightly polluted waters may be taken as an indication that the various chemical elements introduced into the natural waters, are being

transported at different speeds. The reason for this differential interaction with the geological basement is at present still uncertain in its details, although heavy metals complexation by organic ligands is envisaged to be the privileged mechanism to explain such effect.

Acknowledgements

References

Bjerg, P.L., Albrechtsen, H-J., Kjeldsen, P., Christensen, T.H. and Cozzarelli, I. (2003) 'The groundwater geochemistry of waste disposal facilities', in Lollar, B.S. (Ed.): *Environmental Geochemistry, Treatise on Geochemistry*, Vol. 9, pp.541–612.

Christensen, T.H., Kjeldsen, P., Bjerg, P.L., Jansen, D.L., Christensen, J.B., Baun, A., Albrechtsen, H-J. and Heron, J. (2001) 'Biogeochemistry of leachate plumes', *Applied Geochemistry*, Vol. 16, pp.659–718.

Fraser, D.C. (1969) 'Contouring of VLF-EM data', *Geophysics*, Vol. 34, pp.958–967.

Gonçalves, M.A., Cerqueira, L., Figueiras, J. and Putnis, C.V. (2002) 'Use of μ-PIXE and SEM to study metal adsorption and artificial solid phases in polluted environmental samples', in Bruno, J. and Yardley, B.W. (Eds.): *EURESCO Conferences – Geochemistry of Crustal Fluids*, pp.79, 80.

Gonçalves, M.A., Nogueira, J.M.F., Figueiras, J., Putnis, C.V. and Almeida, C. (2004) 'Base-metals and organic content in stream sediments in the vicinity of a landfill', *Applied Geochemistry*, Vol. 19, pp.137–151.

Hirner, A.V. (1992) 'Trace element speciation in soils and sediments using sequential chemical extraction methods', *Intern. J. Environ. Anal. Chem.*, Vol. 46, pp.77–85.

Hirner, A.V. (1996) 'Testing metal mobility in soils by elution tests', in Reuther, R. (Ed.): *Geochemical Approaches to Environmental Engineering of Metals*, Springer-Verlag, Berlin, pp.15–23.

Loke, M.H. and Barker, R.D. (1996) 'Rapid least-squares inversion of apparent resistivity pseudosections by a quasi-Newton method', *Geophys. Prosp.*, Vol. 44, pp.131–152.

Manning, D.A.C. (2001) 'Calcite precipitation in landfills: an essential product of waste stabilization', *Mineralogical Magazine*, Vol. 65, pp.603–610.

Marques, F.O., Mateus, A. and Tassinari, C. (2002) 'The late variscan fault network in central–Northern Portugal (NW Iberia): a re-evaluation', *Tectonophysics*, Vol. 359, pp.255–270.

Marques, F.O., Mateus, A., Amaral, H., Gonçalves, M.A., Tassinari, C., Silva, P. and Miranda, J.M. (2001) 'The amares basin: an ENE-WSW graben formed by recent reactivation of the late-variscan fracture network?', *Comun. Inst. Geol. e Min.*, Vol. 88, pp.33–50.

Mateus, A., Gonçalves, M.A., Marques, F.O. and Monteiro Santos, F. (2003) *Multi-Scale Geometrical Analysis of Fracture Networks in Granite Massifs and its Application to Landfill Site Selection*, A Geologia de Engenharia e os Recursos Geológicos, Coimbra, 2003, Submitted.

Monteiro Santos, F.A., Mateus, A., Marques, F.O. and Gonçalves, M.A. (2006) 'Mapping groundwater contamination around a landfill facility using the VLF-EM method – a case study', *J. Applied Geophysics*, Vol. 60, pp.115–125.

Mota, R., Monteiro Santos, F.A., Mateus, A., Marques, F.O., Gonçalves, M.A., Figueiras, F. and Amaral, H. (2004) 'Granite fracturing and incipient pollution beneath a recent landfill facility as detected by geoelectrical surveys', *J. Applied Geophysics*, Vol. 57, pp.11–22.

Parkhurst, D.L. and Appelo, C.A.J. (1999) *User's Guide to PHREEQC (Version 2) – A Computer Program for Speciation, Batch-Reaction, One-Dimensional Transport, and Inverse Geochemical Calculations*, Water-Resources Investigations Report 99-4259, USGS Denver – Colorado, p.312.

Pohland, F.G. and Kim, J.C. (2000) 'Microbially mediated attenuation potential of landfill bioreactor systems', *Water Science and Technology*, Vol. 41, pp.247–254.

Schwartzenbach, R.P., Gschwend, P.M. and Imboden, D.M. (2003) *Environmental Organic Chemistry*, Wiley-Interscience, New York, p.1313.

Sheppard, D.S., Claridge, G.G.C. and Campbell, I.B. (2000) 'Metal contamination of soils at Scott Base, Antarctica', *Applied Geochemistry*, Vol. 15, pp.513–530.

Stengele, R.H. and Plötze, M. (2000) 'Suitability of minerals for controlled landfill and containment', in Vaughan, D.J. and Wogelius, R.A. (Eds.): *Environmental Mineralogy*, Eötvös University Press, Budapest, Vol. 2, pp.291–331.

Tessier, A., Campbell, P.G.C. and Bisson, M. (1979) 'Sequential extraction procedure for the speciation of particulate trace metals', *Anal. Chem.*, Vol. 51, pp.844–851.

Ure, A.M. (1995) 'Methods of analysis for heavy metals in soils', in Alloway, B.J. (Ed.): *Heavy Metals in Soils*, 2nd ed., Blackie Academic and Professional, London, pp.58–102.